LETTER TO THE EDITOR

Cryo-EM structure of human lysosomal cobalamin exporter ABCD4

Dear Editor,

Cobalamin, also known as vitamin B12, can only be biosynthesized by certain bacteria and archaea. As an essential nutrient for humans, it should be obtained from daily food.[1] Exogenous cobalamin is taken up by the cell through an endocytosis process, then released into the lysosome as a free form, and finally pumped out to the cytosol for utilization.[2] The human ATP-binding cassette (ABC) transporter ABCD4 localized on lysosomal membrane is indispensable for the efflux of cobalamin from lysosome to cytosol.[3] Mutations in ABCD4 gene may result in cobalamin deficiency and inborn diseases. The patients suffer from combined symptoms: hypotonia, lethargy, poor feeding, bone marrow suppression, macrocytic anemia, and heart defects.[3] However, the absence of the structure of human ABCD4 limits our understanding of the molecular mechanism of pathogenesis.

The 606-aa-long human ABCD4 consists of a transmembrane domain (TMD) with six transmembrane (TM) helices followed by a nucleotide-binding domain (NBD). Based on the phylogenetic distance, ABCD4 was classified into the subfamily D, one of seven subfamilies that consist of 48 members of human ABC proteins.[4] Expression and purification of the recombinant full-length human ABCD4 in HEK 293F cells are described in Supplementary information, Data S1. The protein appeared to be stable and homogeneous after extraction and purification in detergent micelles (Supplementary information, Figs. S1a and 2a). The purified protein samples reconstituted into liposomes were subjected to ATPase activity assay. The maximal ATPase activity (V_{max}) of ABCD4 is 11.8 nmol/min/mg (Supplementary information, Fig. S1b), which is comparable to that in the previous report.[5] Using single-particle cryogenic electron microscopy (cryo-EM), we solved the structure of human ABCD4 in the presence of ATP, with the catalytic residue Glu549 substituted by glutamine. After several rounds of iterative 2D and 3D classification and refinement, the overall resolution of the EM map was calculated to 3.6 Å out of 276,557 selected particles according to the gold-standard Fourier shell correlation (FSC) 0.143 criterion (Supplementary information, Figs. S2b–d and 3; Table S1). The EM density exhibits prominent side-chain features in the core region of ABCD4 homodimer that allow us to unambiguously register the residues for all 12 TM helices and the core regions of NBDs (Supplementary information, Figs. S2e and 4). The final model composed of residues Arg13-Lys604, except for a 27-aa linker region (residues Lys357-Ala383), was refined against the EM density to an excellent geometry and statistics (Supplementary information, Fig. S2f and Table S1).

The overall structure of ABCD4 revealed a lysosome-open conformation, with two ATP molecules binding to the interface between two NBDs that are localized in the cytosol (Fig. 1a). Remarkably, most human ABC exporters are localized on the cell membrane that allow both the substrate and ATP to access from the cytosolic side, the so-called cis-side of NBD, thus termed cis-acting exporters.[6] In contrast, human ABCD4 represents a unique exporter that effluxes the substrate in a trans-acting

manner, different from the classic cis-acting exporters. Each TMD contains six helices with significant cytosolic extensions, a hallmark of type I exporters. The TM helices pack against each other closely at the cytosolic side, and diverge into two discrete "wings" facing the lysosomal matrix, thus exhibiting a lysosome-open conformation. Due to domain swapping, each "wing" consists of TM1 and TM2 from one subunit packing against helices 3–6 from the other subunit (Fig. 1b).
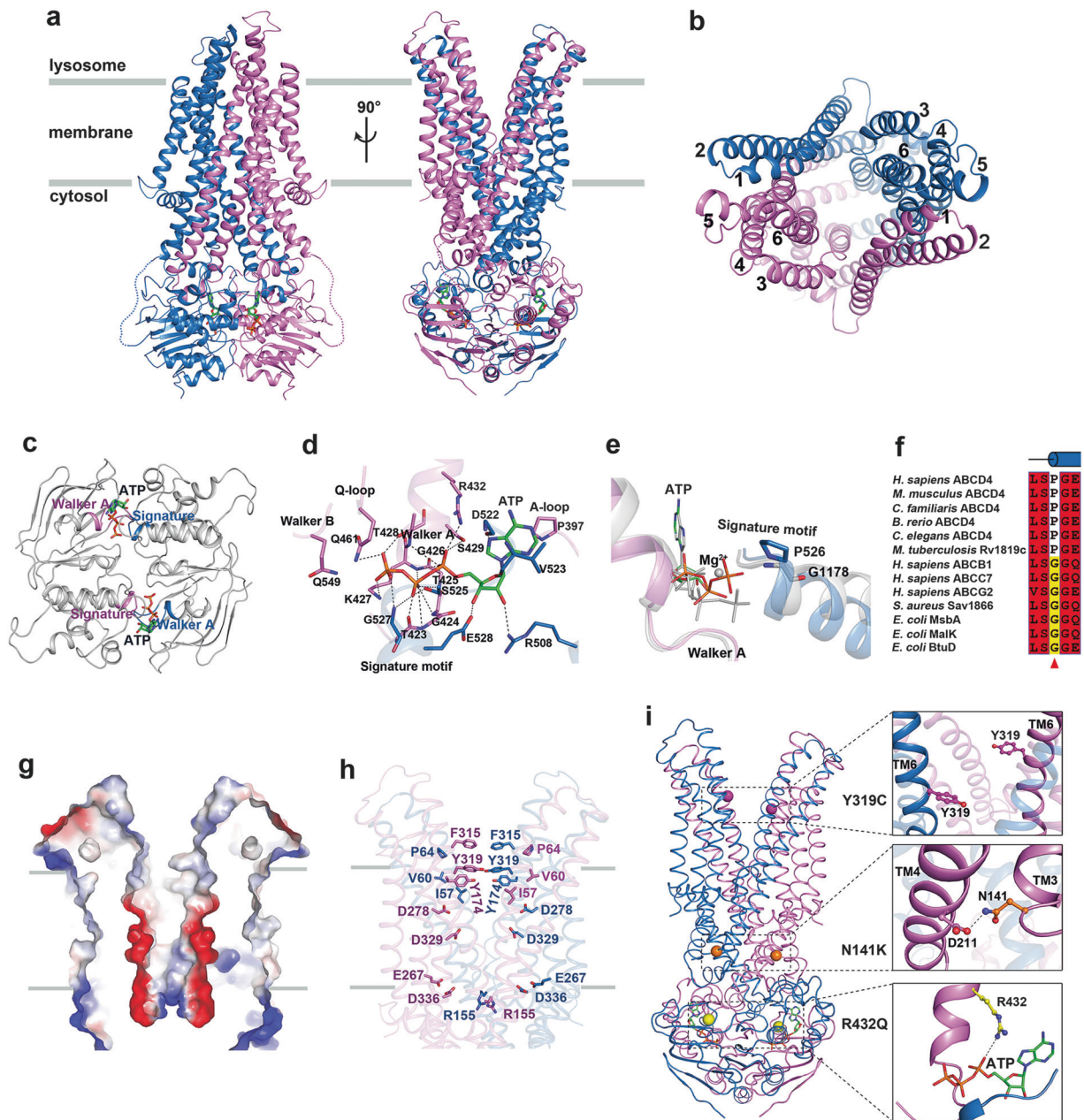
The two NBDs at the cytosolic side form a typical head-to-tail dimer via extensive contacts. At the dimeric interface, we found two ATP molecules, each of which is stabilized by the Walker A motif of one NBD and the ABC signature motif of the other (Fig. 1c). Notably, the magnesium ion was not observed in our structure, similar to a previous report of ABC transporter.[7] The adenine ring of ATP is stacked by two hydrophobic residues Pro397 and Val523, whereas the ribose moiety is stabilized by Arg508 and Glu528 via hydrogen bonds (Fig. 1d). The three phosphate groups mainly interact with the residues from Walker A motif, Q-loop, and signature motif through a network of hydrogen bonds.

Remarkably, ABCD4 possesses an ABC signature motif of LSPGE, rather than the canonical LSGGQ. In the case of ABCB1 (PDB code: 6C0V), the small residue Gly1178 at the very N-terminus is key to the long helix to direct a positively charged helical dipole toward the γ-phosphate of ATP.[6,8] Thus, we propose that replacement of the small residue with a proline in ABCD4 should interfere with the helical dipole interaction (Fig. 1e), which may result in a relatively lower ATPase activity of ABCD4, compared to other ABC exporters.[9–11] Sequence homology search enabled us to reveal that this proline exists not only in eukaryotic ABCD4, but also in some putative cobalamin transporters from prokaryotes. Multiple-sequence alignment further indicated that ABCD4 and homologs possess a distinct proline-containing signature motif (Fig. 1f).

Dissection of electrostatic surface potential of the TMDs showed that the transmembrane cavity starts with an entrance composed of hydrophobic residues, extends to the cytosolic side through a narrowing cleft consisting of four pairs of negatively charged residues, and finally gets closed at the boundary of membrane (Fig. 1g). The hydrophobic entrance is constituted of residues Ile57, Val60, Pro64 from TM1, Thr155, Tyr174 from TM3, and F315, Tyr319 from TM6 (Fig. 1h), similar to the substrate entrance at the TMDs of Escherichia coli vitamin B12 ABC importer BtuCD.[12] In fact, an open hydrophobic cavity was proposed to accommodate the corrin ring moiety of vitamin B12.[13] Moreover, a pair of positively charged residues, namely Arg155 in ABCD4, at the bottom of the cavity are complementary in charge to the phosphate groups of lipid bilayer (Fig. 1h), similar to those in the previously reported structures.[6,14]

Some mutations in ABCD4 gene result in cobalamin deficiency and severe diseases. The present structure of ABCD4 enabled us to elucidate the molecular basis of pathogenesis due to these mutations. To date, seven clinical mutations in ABCD4 gene have

Fig. 1 Cryo-EM structure of human lysosomal cobalamin exporter ABCD4. **a** The structure of ABCD4 in a lysosome-open state is shown in two perpendicular views with cartoon representation. The two monomers are colored in violet and blue, respectively. ATP molecule is shown in sticks and colored by elements. **b** A top view of ABCD4 from the inside of lysosome. The six TM helices of each monomer are indicated by numbers. **c** The NBD of ABCD4 adopts a head-to-tail state with ATP sandwiched between Walker A motif of one NBD and ABC signature motif of the other. The NBD is colored in light gray. The Walker A motif and ABC signature motif of each monomer are colored in violet and blue, respectively. ATP is shown as sticks. **d** ATP-binding pattern of ABCD4. Residues at the ATP-binding site are shown as sticks. Hydrogen bonds and ionic interactions between ABCD4 and ATP are indicated by dash lines. **e** Superposition of ATP-binding sites of ABCB1(PDB code: 6C0V) and ABCD4. Pro526 and Gly1178 in the signature motifs of ABCD4 and ABCB1, are shown as sticks, respectively. The ABCB1 and ATP molecule in ABCB1 are both colored in light gray. **f** Multiple-sequence alignment of the signature motifs. Sequences include human ABCD4 and homologs from *Mus musculus, Canis familiaris, Brachydanio rerio*, and *Caenorhabditis elegans*, and the putative cobalamin transporter Rv1819c in *Mycobacterium tuberculosis*, as well as human ABCB1, ABCC7, and ABCG2, Sav1866 in *Staphylococcus aureus*, and the *E. coli* MsbA, MalK, and BtuD. **g** A section view for the electrostatic surface potential of the substrate cavity in ABCD4, colored by electrostatic potential ranging from blue (most positive) to red (most negative). **h** Residues at the substrate cavity shown as sticks. **i** Mapping of three clinically identified pathogenic mutations, N141K, F319C, and R432Q to ABCD4 structure. The Cα atoms of the indicated residues are shown as spheres. Close-up views of the local structure around Tyr319, Asn141, and Arg432 are shown on right

been deposited in Human Gene Mutations Database (http://www.hgmd.cf.ac.uk), including two in-frame deletions, two frame-shifts, and three missense mutations N141K, Y319C, and R432Q. One in-frame deletion of the coding region corresponding to residues Asp143-Ser181 results in the missing of TM3 helix, which

contributes to the formation of the substrate cavity of ABCD4. The other in-frame deletion of a region encoding residues Gly443-Ser485 leads to the absence of Q-loop and flanking regions of NBD that interacts with the coupling helix. Both the two frame-shift mutations, one with a dinucleotide CT insertion and the other

with a dinucleotide AG deletion, introduce a premature stop codon, and lead to the mis-translation of succeeding residues in addition to truncation of the C-terminal β-strands of the RecA-like subdomain of NBD. The absence of either TM3, Q-loop or the C-terminal β-strands of NBD will result in the inactivation or instability of ABCD4.

More importantly, the three point mutations could be clearly mapped to our structure (Fig. 1i). The side chain of Tyr319, which points towards the substrate cavity, may contribute to the hydrophobic interaction with the corrin ring of cobalamin. Once Tyr319 is mutated to cysteine, it will change the local hydrophobicity, thus altering the substrate binding affinity. Moreover, as exposed to an oxidized micro-environment in lysosome, the two cysteine residues are prone to forming a disulfide bond once the two TMDs get close to each other, thus maintaining ABCD4 in a constitutively closed conformation. In the case of N141K mutation, the hydrogen bond between Asn141 and Asp211 will be altered. For the third point mutation, as the residue Arg432 is responsible for binding to the α-phosphate of ATP, an R432Q mutation will alter the interaction, and might reduce the ATPase activity. Notably, the three residues Tyr319, Asn141, and Arg432 are highly conserved in all putative cobalamin exporters (Supplementary information, Fig. S5a), indicating their indispensable role in the transport function of ABCD4 and homologs. Moreover, both Y319C and R432Q mutants exhibited much lower ATPase activities compared to the wild-type ABCD4 (Supplementary information, Fig. S5b); the mutant N141K could not be overexpressed. All together, the present cryo-EM structure of ABCD4 not only deciphered the molecular insights of diseases caused by the currently known mutations, but also provided a framework to assess the lethality of *ABCD4* gene mutations that will be identified clinically in the future.

In sum, we present here the cryo-EM structure of human ABCD4 in the ATP-bound and lysosome-open conformation, representing the first structure in human ABCD subfamily. As localized on the membrane of lysosome, it adopts a *trans*-acting transport mechanism distinct from other type I exporters of known structure. Moreover, a unique ABC signature motif makes ABCD4 the founding member of a new family of ABC transporters. Mapping of clinically identified mutations to our structure provides molecular insights into the pathogenesis. These findings not only advance our understanding of the molecular mechanism of ABC transporters, but also give hints for the further therapeutic intervention of related human diseases.

DATA AVAILABILITY

All relevant data are available from the authors and/or included in the manuscript. Atomic coordinates and EM density maps of the human ABCD4 have been deposited in the Protein Data Bank (PDB code: 6JBJ) and the Electron Microscopy Data Bank (EMDB code: EMD-9791), respectively.

AUTHOR CONTRIBUTIONS

C.-Z.Z. and Y.C. conceived the project and planned the experiments. D.X. expressed and purified human ABCD4. D.X., Z.F., and W.-T.H. performed functional assays. Z.F. performed initial negative-stain and cryo-EM analyses and prepared all grids. D.X. and Z.F. performed cryo-EM data collection. D.X. performed ABCD4 structure determination and Z.F. built the ABCD4 model. Y.-L.J. and L.S. revised the model, and Z.F. performed model refinement. D.X., Z.F., L.S., C.-Z.Z., and Y.C. wrote the manuscript; all authors contributed to the revision.

ADDITIONAL INFORMATION

Da Xu[1], Zhang Feng [iD][1], Wen-Tao Hou[1], Yong-Liang Jiang[1], Liang Wang[1], Linfeng Sun[1,2], Cong-Zhao Zhou [iD][1] and Yuxing Chen[1]

[1]*Hefei National Laboratory for Physical Sciences at the Microscale and School of Life Sciences, University of Science and Technology of China, 230027 Hefei, Anhui, China and* [2]*CAS Centre for Excellence in Molecular Cell Science, University of Science and Technology of China, 230027 Hefei, Anhui, China*
These authors contributed equally: Da Xu, Zhang Feng.
Correspondence: Linfeng Sun (sunlf17@ustc.edu.cn) or Cong-Zhao Zhou (zcz@ustc.edu.cn) or Yuxing Chen (cyxing@ustc.edu.cn)

REFERENCES

1. Watanabe, F. *Exp. Biol. Med.* **232**, 1266–1274 (2007).
2. Nielsen, M. J., Rasmussen, M. R., Andersen, C. B., Nexø, E. & Moestrup, S. K. *Nat. Rev. Gastroenterol. Hepatol.* **9**, 345–354 (2012).
3. Coelho, D. et al. *Nat. Genet.* **44**, 1152–1155 (2012).
4. Dean, M., Hamon, Y. & Chimini, G. *J. Lipid Res.* **42**, 1007–1017 (2001).
5. Okamoto, T. et al. *Biochem. Biophys. Res. Commun.* **496**, 1122–1127 (2018).
6. Ter Beek, J., Guskov, A. & Slotboom, D. J. *J. Gen. Physiol.* **143**, 419–435 (2014).
7. Caffalette, C. A., Corey, R. A., Sansom, M. S. P., Stansfeld, P. J. & Zimmer, J. *Nat. Commun.* **10**, 824 (2019).
8. Kim, Y. & Chen, J. *Science* **359**, 915–919 (2018).
9. Zhang, Z. & Chen, J. *Cell* **167**, 1586–1597 (2016).
10. Johnson, Z. L. & Chen, J. *Cell* **168**, 1075–1085 (2017).
11. Qian, H. et al. *Cell* **169**, 1228–1239 (2017).
12. Locher, K. P., Lee, A. T. & Rees, D. C. *Science* **296**, 1091–1098 (2002).
13. Furger, E., Frei, D. C., Schibli, R., Fischer, E. & Prota, A. E. *J. Biol. Chem.* **288**, 25466–25476 (2013).
14. Ho, H. et al. *Nature* **557**, 196–201 (2018).